Noninvasive characterization of the fission yeast cell cycle by monitoring dry mass with digital holographic microscopy

Benjamin Rappaz
Ecole Polytechnique Fédérale de Lausanne
Brain Mind Institute
CH-1015 Lausanne, Switzerland

Elena Cano
Ecole Polytechnique Fédérale de Lausanne
ISREC
CH-1015 Lausanne, Switzerland

Tristan Colomb
Lyncée Tec SA
PSE-A
CH-1015 Lausanne, Switzerland

Jonas Kühn
Christian Depeursinge
Ecole Polytechnique Fédérale de Lausanne
Imaging and Applied Optics Institute
CH-1015 Lausanne, Switzerland

Viesturs Simanis
Ecole Polytechnique Fédérale de Lausanne
ISREC
CH-1015 Lausanne, Switzerland

Pierre J. Magistretti
Ecole Polytechnique Fédérale de Lausanne
Brain Mind Institute
CH-1015 Lausanne, Switzerland

Pierre Marquet
Ecole Polytechnique Fédérale de Lausanne
Brain Mind Institute
CH-1015 Lausanne, Switzerland
    and
Centre de neurosciences psychiatriques
Département de psychiatrie DP-CHUV
Site de Cery
CH-1008 Prilly-Lausanne, Switzerland

Abstract. Digital holography microscopy (DHM) is an optical technique which provides phase images yielding quantitative information about cell structure and cellular dynamics. Furthermore, the quantitative phase images allow the derivation of other parameters, including dry mass production, density, and spatial distribution. We have applied DHM to study the dry mass production rate and the dry mass surface density in wild-type and mutant fission yeast cells. Our study demonstrates the applicability of DHM as a tool for label-free quantitative analysis of the cell cycle and opens the possibility for its use in high-throughput screening. © *2009 Society of Photo-Optical Instrumentation Engineers.* [DOI: 10.1117/1.3147385]

1 Introduction

Most cells reproduce by duplicating their content and then dividing to produce daughters of equal size. The ability to genetically manipulate yeast cells, coupled with their rapid growth rate, has made them an attractive model to study cell growth and division.[1] Many genes affecting these processes have been identified[2] and have revealed the basic mechanisms controlling cell division.

Cells of the fission yeast *Schizosaccharomyces pombe* (*S. pombe*) may be considered as cylinders capped by hemispherical ends; they grow mainly by tip-elongation and divide by formation of a medially placed septum, which is cleaved to produce two daughter cells. Cell elongation stops upon commitment to mitosis, when the cell wall synthesis machinery is reorganized from the tips to the medial region, where the di-

Address all correspondence to: Benjamin Rappaz, EPFL, LNDC-BMI-SV – Station 15, Lausanne, VD 1015 Switzerland. Tel: 41 21 6939524; E-mail: benjamin.rappaz@mcgill.ca
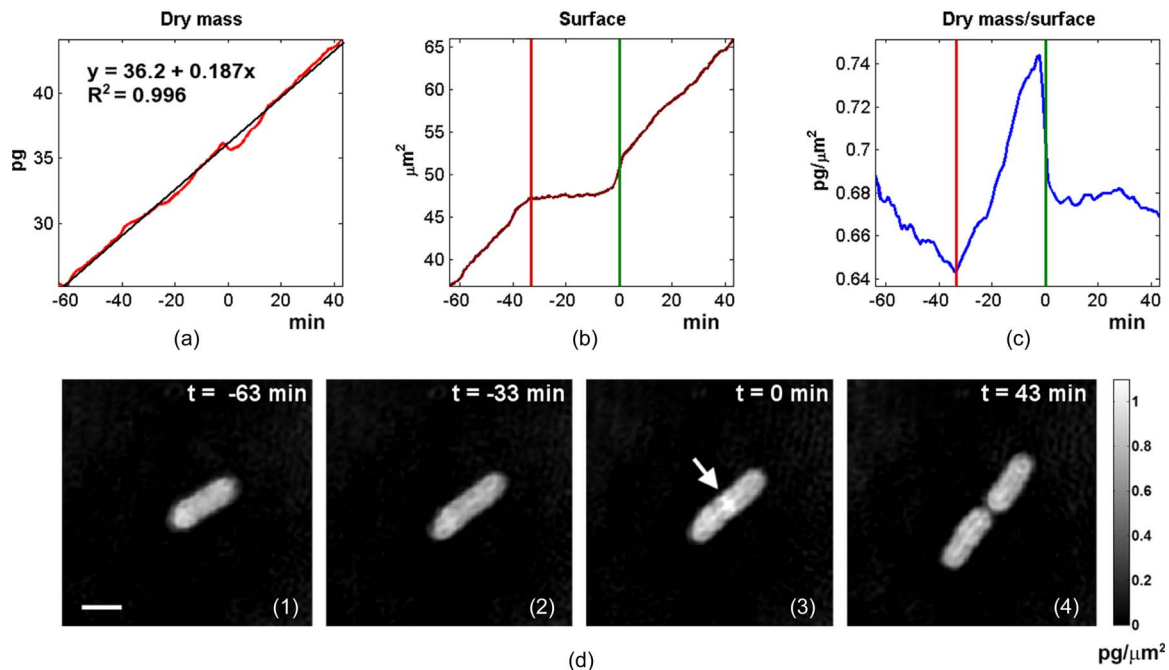
Fig. 1 Time evolution of: (a) dry mass (fit: linear regression), (b) projected cell surface, and (c) DM concentration. Vertical lines: red, end of surface growth; green, cytokinesis. (d) Representative DM surface density images recorded at the beginning (1), at the end of cell growth (2), just before cytokinesis (arrow: septum) (3), and at the end of the recording period (4). Scale bar 5 μm. The two sister cells after cell division have been considered as a single cell in order to coherently appreciate the evolution of the measured parameters. The results are representative of five wild-type cells. (Color online only.)

vision septum forms at the end of mitosis. After cytokinesis, growth resumes at the pre-existing (old end) before switching to bipolar growth during G2 (see Ref. 3 for a review). Thus, the length of an *S. pombe* cell is directly proportional to its volume during interphase.[4]

Cells need to double their content during each cell cycle to preserve a constant size. A good indicator of the biomass is the dry mass (nonaqueous material), defined as the weight of the cell when water has evaporated and which mainly depends on protein concentration.[5] Thus, monitoring the dry mass production provides a dynamic indicator of the real-time evolution of the cell cycle.

Using interferential microscopy, Barer proposed a method[5] to relate the measured quantitative phase shift induced by the observed cell on the transmitted light wave front to the dry mass. This relationship has been used by Zicha and Dunn[6] to study the spreading of fibroblast with a DRIMAPS system (digitally recorded interference microscopy with automatic phase shifting); however, this analysis required the acquisition of four interferograms and extensive postprocessing of the data.

Recently,[7–10] novel quantitative phase microscopy (QPM) techniques have been used to measure cell-induced phase shift, thus allowing the analysis of cell structure and dynamics. The QPM that we have developed, called digital holographic microscopy (DHM), has the ability to explore cell dynamics by providing, from a single recorded hologram, a quantitative phase image of a living cell with a nanometric axial sensitivity.[9,11] This method of numerical processing of holograms allows us not only to reconstruct quantitative phase images,[12] but also to compensate for aberrations due to ex-

perimental noise (time drift, vibration, etc.) and to perform off-line numerical refocusing.[13] This assures a high level of phase stability, thus making it possible to explore biological processes occurring on a day-to-millisecond time scale.

Within the framework of QPM, Barer's relationship has recently been used by Popescu et al.[14] to investigate cell mass and growth dynamics. In this paper, we have applied DHM to provide a noninvasive, dynamic measurement of the dry mass production rate and cell density changes during the *S. pombe* cell cycle.

2 Materials and Methods

The transmission DHM and phase image reconstruction techniques used for the present study have been described in Refs. 9, 12, and 13. *S. pombe* were grown according to standard methods in Y5 complete medium[15] to early log-phase and then mounted on coverslips for imaging. Experiments with the wild-type strain 972 h- and with a temperature-sensitive *cdc16-116 h+* were conducted at 36 °C (nonpermissive temperature for the cell cycle mutant). The microscope was placed in a closed Plexiglas box ("the Cube" system, Life Imaging Services, Switzerland). The cell chamber was further heated at 36 °C with a custom-made PID-controlled thermoresistance to ensure that a stable temperature was maintained throughout the experiment.

Barer[5] showed that the phase shift induced by a cell is related to its dry mass (DM) by the following equation (converted to the International System of Units):
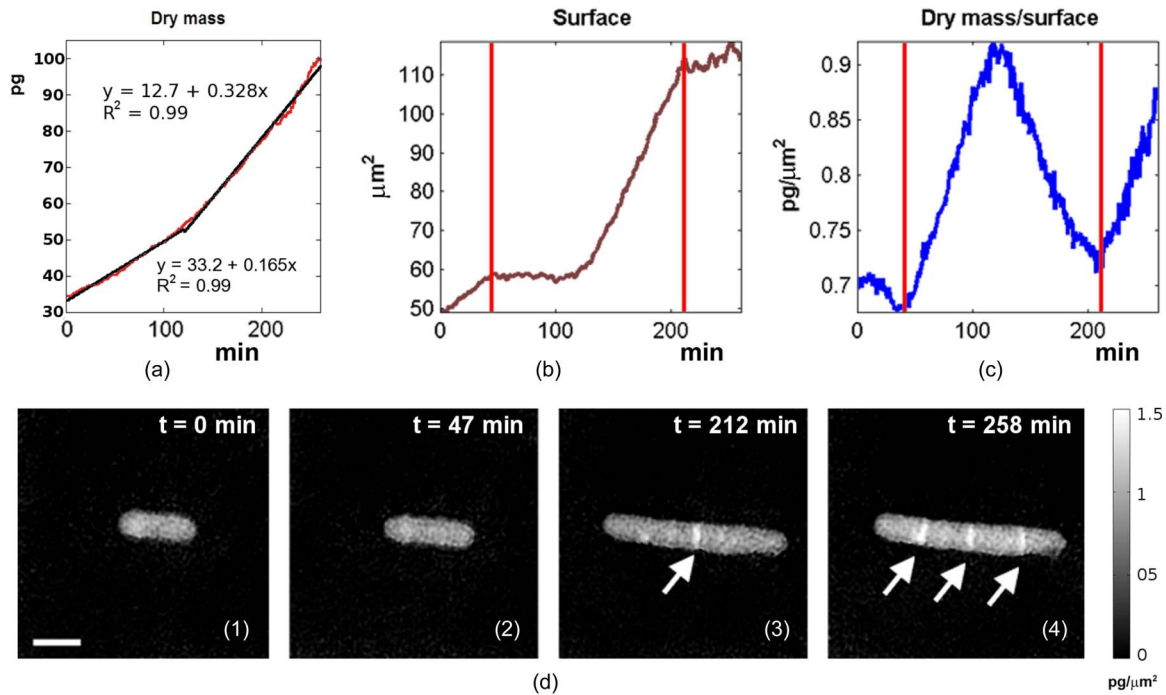
Fig. 2 Time evolution of: (a) dry mass (fit: two linear regressions), (b) cell surface, and (c) DM concentration. Vertical red line: end of surface growth. (d) representative dry mass density images recorded at the beginning (1), at the first end of cell growth (2), at the second end of cell growth (3), and at the end of the recording period (4). Arrows indicate septum position. Scale bar 5 μm. (Color online only.)

$$DM = \frac{10\lambda}{2\pi\alpha}\int_{S_c}\Delta\varphi ds = \frac{10\lambda}{2\pi\alpha}\Delta\bar{\varphi}S_c, \qquad (1)$$

where $\Delta\bar{\varphi}$ is the mean phase shift induced by the whole cell, λ is the wavelength of the light source of the setup (663 nm), S_c is the projected cell surface (determined by a homemade watershed edge-detection algorithm), and α is a constant known as the specific refraction increment (in cubic meters per kilogram) related to the intracellular content. α can be approximated by $0.0018-0.0021$ m^3/Kg, when considering a mixture of all the components of a typical cell.[5]

3 Results and Discussion

3.1 *Wild-Type Cells*

We began by analyzing the dry mass surface density (DMSD) of wild-type cells (strain 972 h^-). Changes in the DM through the cell cycle were obtained by recording the mean phase shift of the cell and its projected surface according to Eq. (1).

The results obtained from analysis of five cells are presented in Fig. 1, which shows the change in the DM (pg), projected cell surface, and DM surface density (DMSD in pg/μm^2), defined as the ratio of the last two quantities, through the cell cycle. Four DMSD images of a cell at various stages of the division cycle are shown. The region where the septum forms Fig. 1(d)(3) has a high DM density (>1pg/μm^2), which probably reflects the recruitment of proteins and carbohydrates involved in the synthesis and subsequent cleavage of the division septum.

Figure 1(a) shows a constant production rate of DM at around 10.7 pg/h (as indicated by linear regression) during the whole cell cycle; a mean value of 11.1 ± 1.5 pg/h

[mean $\pm$ standard error of the mean, (SEM)] was found for five wild-type cells. This production rate predicts that the cell should doubles its protein content in about 2.3 h, which is consistent with the doubling time of fission yeast at 36 °C reported by a study of *S. pombe* growth by Mitchison[4] using a Baker interference microscope.

The cell surface exhibits linear growth during interphase and is followed by a nongrowing period of 35 min (indicated by the green vertical line) before cytokinesis when cells enter mitosis (see Introduction).

Specific variations of the DMSD were observed through the cell cycle. At first, the DMSD slowly declines, indicating a larger surface growth than dry mass production. In contrast, during the 35 min preceding cytokinesis, as the DM production remains constant and the surface growth pauses, the DMSD showed a significant increase with a maximum value occurring a few minutes before the cytokinesis. This peak value is likely related to the recruitment and/or synthesis of components involved in the mitosis, cytokinesis, and the subsequent S-phase, which occurs prior to cell separation.[4] As cells divide, the rapid surface increase and the septum degradation induce an abrupt decrease in DMSD [Fig. 1(c), green line].

3.2 *Cdc16-116 Mutant*

We have also characterized the DM, cell surface, and DMSD parameters in a *cdc16-116* mutant.[16] *Cdc16p* is required to limit the cell to a single septum per cell cycle; if it is inactivated, the cell synthesizes multiple additional septa, producing anucleate cell compartments,[16] cf. Fig. 2(d)(4).

In contrast to the wild-type cells, the production of DM shows a bilinear pattern[17] with linear segments representing
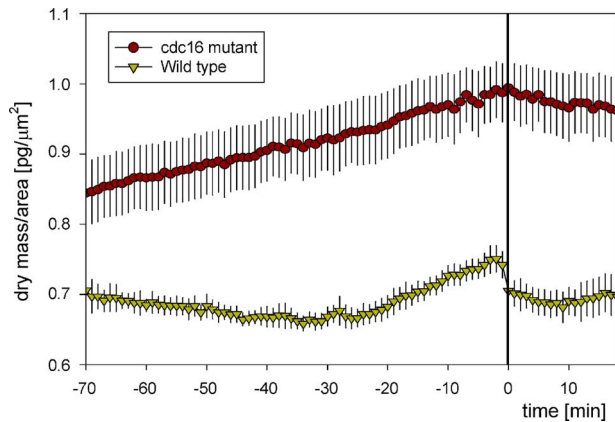
Fig. 3 Comparison of the DM concentration for wild-type (triangle) and *cdc16* mutant (circle) fission yeast. Data expressed as mean±SEM for five cells. The horizontal line denotes time of cytokinesis for wild-type and the stage of maximal DM concentration for mutant.

constant growth rates, separated by a transitional period around a rate-change point (RCP, here at minute 120) during which the rate of growth increases. However, there is considerable controversy concerning the exact time profile of size-related parameters, including length, volume, and surface during the cell cycle, and several models (linear, exponential, bilinear, etc.) have been proposed.[17]

The data for a typical cell presented here show a twofold increase of the DM production rate, from 9.9 to 19.7 pg/h after the RCP, which occurs at the end of the mitotic "plateau" [Fig. 2(b)]. At this time, the two daughter cells are separated by a septum but remain attached to each other.

The mean hour DM production of the *Cdc16-116* mutant cell, 13.8 ± 3.5 pg/h (mean $\pm$ SEM, $n=5$ cells), was found to be slightly higher than the DM production of the wild-type cells. It is possible that this represents the continued accumulation of dense septal material in these cells.

Although the cell surface area of the *cdc16-116* and wild-type yeasts both show alternating plateau and expansion phases, the abrupt change in DSMD that accompanies cell separation in wild-type [Fig. 1(b)] is absent from the *cdc16-116* mutant, which shows a more symmetrical sawtooth pattern. It is likely that the increase occurs while the septa are being synthesized, while cell elongation has stopped, and that the decrease represents a resumption of cell elongation. A more detailed explanation of these data will require a greater understanding of the growth patterns of *cdc16-116* under restrictive conditions.

A comparison of typical wild-type and mutant DSMD time courses (Fig. 3) shows that the DMSD values in *cdc16-116* are approximately 25% larger than wild-type. Although the absence of the rapid postcytokinesis surface enlargement and the persistence of the septum in *cdc16-116* contribute to this difference, DMSD calculations performed before septum formation (or excluding the contribution of additional septa, ~5 pg each) still show a significantly larger DMSD (15%) than for the wild type. The reason for this is unclear at present. It is also important to note that at the end of the cell cycle of the wild-type yeast the dry mass concentration returns to the basal

level [cf. Figs. 1(c) and 2(c)], indicating a homeostasis of the dry mass along generation.

4 Conclusion

We have used DHM to study the DM production rate and DMSD through the cell cycle of wild-type and mutant yeasts at the single-cell level in a noninvasive manner. We have observed that the DM production rate of the mutant and wild-type cells are significantly different, and the wild-type DMSD shows a specific pattern resulting from the cytokinesis process, which is absent in the mutant.

Dry mass accumulation can be combined to other parameters easily measured by DHM, like the volume and refractive index,[11] to provide a better understanding of the cell cycle. DHM technique can thus be further used for high-throughput, label-free screening, allowing a rapid quantitative characterization of the cell cycle and the effects of specific pharmacological agents likely to affect cell cycle progression.

References

1. L. H. Hartwell, J. Culotti, J. R. Pringle, and B. J. Reid, "Genetic control of cell-division dycle in yeast," *Science* **183**(4120), 46–51 (1974).
2. P. Nurse, P. Thuriaux, and K. Nasmyth, "Genetic control of the cell division cycle in the fission yeast *Schizosaccharomyces pombe*," *Mol. Gen. Genet.* **146**(2), 167–178 (1976).
3. S. L. Forsburg and P. Nurse, "Cell-cycle regulation in the yeasts *Saccharomyces-cerevisiae* and *Schizosaccharomyces-pombe*," *Annu. Rev. Cell Biol.* **7**, 227–256 (1991).
4. J. M. Mitchison, "The growth of single cells, 1. *Schizosaccharomyces pombe*," *Exp. Cell Res.* **13**(2), 244–262 (1957).
5. R. Barer, "Interference microscopy and mass determination," *Nature (London)* **169**(4296), 366–367 (1952).
6. D. Zicha and G. A. Dunn, "An image-processing system for cell behavior studies in subconfluent cultures," *J. Microsc.* **179**, 11–21 (1995).
7. D. Carl, B. Kemper, G. Wernicke, and G. von Bally, "Parameter-optimized digital holographic microscope for high-resolution living-cell analysis," *Appl. Opt.* **43**(36), 6536–6544 (2004).
8. C. L. Curl, C. J. Bellair, P. J. Harris, B. E. Allman, A. Roberts, K. A. Nugent, and L. M. Delbridge, "Quantitative phase microscopy: a new tool for investigating the structure and function of unstained live cells," *Clin. Exp. Pharmacol. Physiol.* **31**(12), 896–901 (2004).
9. P. Marquet, B. Rappaz, P. J. Magistretti, E. Cuche, Y. Emery, T. Colomb, and C. Depeursinge, "Digital holographic microscopy: a noninvasive contrast imaging technique allowing quantitative visualization of living cells with subwavelength axial accuracy," *Opt. Lett.* **30**(5), 468–470 (2005).
10. G. Popescu, T. Ikeda, R. R. Dasari, and M. S. Feld, "Diffraction phase microscopy for quantifying cell structure and dynamics," *Opt. Lett.* **31**(6), 775–777 (2006).
11. B. Rappaz, P. Marquet, E. Cuche, Y. Emery, C. Depeursinge, and P. J. Magistretti, "Measurement of the integral refractive index and dynamic cell morphometry of living cells with digital holographic microscopy," *Opt. Express* **13**(23), 9361–9373 (2005).
12. E. Cuche, P. Marquet, and C. Depeursinge, "Simultaneous amplitude-contrast and quantitative phase-contrast microscopy by numerical reconstruction of Fresnel off-axis holograms," *Appl. Opt.* **38**(34), 6994–7001 (1999).
13. T. Colomb, F. Montfort, J. Kuhn, N. Aspert, E. Cuche, A. Marian, F.

Charriere, S. Bourquin, P. Marquet, and C. Depeursinge, "Numerical parametric lens for shifting, magnification, and complete aberration compensation in digital holographic microscopy," *J. Opt. Soc. Am. A* **23**(12), 3177–3190 (2006).

14. G. Popescu, Y. Park, N. Lue, C. Best-Popescu, L. Deflores, R. R. Dasari, M. S. Feld, and K. Badizadegan, "Optical imaging of cell mass and growth dynamics," *Am. J. Physiol.: Cell Physiol.* **295**(2), C538–544 (2008).

15. S. Moreno, A. Klar, and P. Nurse, "Molecular genetic analysis of fission yeast Schizosaccharomyces pombe," *Methods Enzymol.* **194**, 795–823 (1991).

16. M. Minet, P. Nurse, P. Thuriaux, and J. M. Mitchison, "Uncontrolled septation in a cell-division cycle mutant of the fission yeast *Schizosaccharomyces-pombe*," *J. Bacteriol.* **137**(1), 440–446 (1979).

17. P. Buchwald and A. Sveiczer, "The time-profile of cell growth in fission yeast: model selection criteria favoring bilinear models over exponential ones," *Theor. Biol. Med. Model.* **3**, 16 (2006).